C.P. No. 1216

C.P. No. 1216

MINISTRY OF DEFENCE (PROCUREMENT EXECUTIVE)

AERONAUTICAL RESEARCH COUNCIL

CURRENT PAPERS

Fortran Programmes for Axisymmetric Potential Flow Around Closed and Semi-Infinite Bodies

By

C. M Albone, M.Sc

LONDON HER MAJESTY'S STATIONERY OFFICE

1972

Price 65p net

C.P. No.1216*
March 1970

FORTRAN PROGRAMMES FOR AXISYMMETRIC POTENTIAL FLOW AROUND CLOSED AND SEMI-INFINITE BODIES

- by -

C. M. Albone, M.Sc.**

SUMMARY

Two programmes are presented in I.C.L. FORTRAN, for the pressure distribution on the surface of an arbitary body of revolution in axisymmetric, incompressible flow. One programme evaluates the pressure distribution on an arbitary closed body of revolution. The second deals with a body which has a parallel afterbody extending to infinity downstream.

Listings for each programme are given in the Appendicies.

Results from both programmes are presented and their accuracy is demonstrated. The range of bodies for which the programmes work is also shown.

---

* Replaces A.R.C.32 346

** Now in Aerodynamics Dept. R.A.E. Farnborough.

Contents

1. Introduction

The incompressible, irrotational flow of a perfect fluid over a body of revolution whose axis is parallel to a uniform stream is considered. The method and programmes described give only the velocity distribution on the surface of the body and provide no information about the velocity field elsewhere. Landweber has shown (ref 1) that by applying Green's Theorem to the solution of the boundary value problem for velocity potential, an integral equation for the velocity on the body surface can be obtained. For problems in which only the surface distribution of velocity is required this integral equation can be solved more rapidly than other equations so far proposed. Again, Landweber (ref 1) presents an iterative solution of the integral equation for closed bodies of revolution, making use of Gaussian quadrature as an accurate method of performing the numerical integration. This report presents a FORTRAN programme enabling the iterative solution to be computed.

The solution of Landweber is extended to deal with the case of an infinite parallel sided afterbody. Such a solution has two immediate applications:-

(i) for comparison with low speed tunnel measurements of the pressure distribution on the forebody of a sting-mounted model
(ii) for the calculation of the pressure distribution over a body of revolution in well-separated axisymmetric flow (A simple mathematical model for the solution of Laplace's equation in the region exterior to a body and wake is that of a fictitious body extending to infinity downstream)

A FORTRAN Programme for the pressure distribution in the case of an infinite afterbody is also presented.

Since the integral equation for velocity is exact, the accuracy of any solution is governed by that of the numerical integration performed at each stage of the iteration. With Gaussian quadrature, this is very good, especially if many abscissae are used. Both programmes show that there is no difficulty in obtaining convergence to any reasonable degree of accuracy. This is so even in the event of irregular body geometry, such as that of the three-stage rocket for which results are presented. In addition the programmes cope equally well with sharp and blunt nosed bodies. The body geometry required by the programmes is simply the body radius and surface slope at each Gaussian abscissa. These are supplied via a sub-routine, and not input as data, so as to simplify programme handling.

The run times on The City University's I.C.L. 1905 computer are up to two minutes for each body. Most bodies, however are dealt with in a few seconds.

2. Discussion of programme for the closed body

The integral equation for surface velocity (ref 1) derived in appendix A, is

$$\int_0^P \frac{U(x)\,y^2(x)\,ds}{2\,r^3(x,t)} = 1$$

where:-

$$r^2(x,t) = (x-t)^2 + y^2(x)$$

$$ds = dx/\cos\gamma$$

In appendix B the solution of the integral equation is shown to be the limiting form of U_n (as $n \to \infty$). The functions U_n with corresponding error functions E_n are given by:

$$U_1(x) = (1+k_0)\cos\gamma(x) \qquad \text{---------- 22.}$$

$$E_1(t) = 1 - \left(\frac{1+k_0}{2}\right)\int_{X_0}^{X_1}\left[k(x,t) - k'(x,t)\right]dx - \frac{1+k_0}{1+k_1(t)} \qquad \text{----33.}$$

and

$$E_{n+1}(t) = E_n(t)\left[\frac{E_1(t)+k_0}{1+k_0}\right] - \frac{1}{2}\int_{X_0}^{X_1} k(x,t)\left[E_n(x) - E_n(t)\right]dx \qquad \text{--36.}$$

$$U_{n+1}(t) = U_1(t) + \cos\gamma(t)\sum_{i=1}^{n} E_i(t) \qquad \text{---------26.}$$

The quantities contained in these expressions are fully described in appendix B.

The integrals occurring in the expressions for $E_n(t)$ $n \geq 1$ must be reduced so that their limits are -1 to +1 in order to apply Gaussian quadrature. A linear transformation

$$x' = \frac{2x - (X_0+X_1)}{(X_1 - X_0)}$$

gives limits of -1 and +1 on x^1 corresponding to x_0 and x_1 on x.

Substituting into the integrals and suppressing the dashes one obtains:-

$$E_1(t) = 1 - \frac{(1+k_0)(x_1-x_0)}{4}\int_{-1}^{+1}\left[k(x,t)-k'(x,t)\right]dx \quad - \frac{1+k_0}{1+k_1(t)}$$

$$E_{n+1}(t) = E_n(t)\left[\frac{E_1(t)+k_0}{1+k_0}\right] - \left(\frac{x_1-x_0}{4}\right)\int_{-1}^{+1} k(x,t)\left[E_n(x)-E_n(t)\right]dx$$

The programme for the solution of these four equations written in I.C.L. FORTRAN is listed in appendix C.

Input arrangement and layout of results

For a given body geometry, the accuracy of the solution depends upon two factors:-

(i) the value of $\max\{E_n(t)\}$ at which the computation is halted

(ii) the order of the Gaussian quadratures. The first of these two is set as data to any required value (usually of the order of 10^{-3} to 10^{-4}.) The second factor presents more of a problem regarding ease of programme handling. Leaving the number of abscissae arbitary (i.e. to be set as data) requires a set of Gaussian weights and abscissae to be input, at each run, corresponding to that number. This is a rather cumbersome arrangement which would be overcome if the number of abscissae was kept constant. Sixteen point quadrature was thought by Landweber to give good results for most bodies. In the case of bodies with regions of high curvature, this number could well be greater with advantage. For the form of the programme presented here it has been decided to keep the number of points fixed at 40 and to include the list of weights and abscissae in the programme. This number is sufficient for almost all body geometries and clearly will provide superfluous information for simple bodies. However, the justification for fixing this number so high is that run times even with 40 points are only of the order of seconds.

A further simplification in handling the data is achieved by building in a simple subroutine to evaluate y and dy/dx at each of the 40 points on the body. It will be necessary for the user to write two or three lines of FORTRAN to form these two quantities at any position x on the particular body under investigation.

The amount of data to be supplied now reduces to five numbers.

(i) NMAX - the maximum number of iterations permitted (used as a safeguard should convergence not be achieved or be slower than expected)
A typical value is 100.

(ii) EPS - convergence achieved only if $|\max\{E_n(t)\}|$ is less than EPS.
A typical value is 0.0001

(iii) xx0 - the nose abscissa, x_0

(iv) xx1 - the tail abscissa, x_1

(v) yMID - the value of y at the mid-point of the body
i.e. at $x = \frac{1}{2}(x_0 + x_1)$

Example:- $y = 0.2\,x(1 - x)$, a 10% thick parabolic arc of revolution. The data card consists of the five numbers (the first being of type integer, the other four being real) each separated by a space.

```
100 0.0001 0.0 1.0 0.05
```

The two lines of FORTRAN to be written to give y and dy/dx are:-

```
FB = 0.2 * XB * (1.0 - XB)

F1B = 0.2 - 0.4 * XB
```

These are placed in the Subroutine BODY.

The output is headed by a statement of the number of iterations and the maximum value of the error function at the time the computation ceased. This is followed by five columns of 40 numbers. These are x, y, dy/dx, U and C_p at the 40 abscissae. The surface velocity (non-dimensionalised by the velocity in the free stream) and the pressure coefficient are given to 4 decimal places.

(Since none of the Gaussian abscissae actually falls at $x = x_0$ or $x = x_1$, a body having an infinite value of dy/dx, at the nose or tail presents no problems. For such a blunt nosed body, the value of dy/dx, at the abscissa nearest the nose, would be large, but finite)

3. Discussion of programme for a body extending to infinity

The four equations for the iterative solution of Landweber's integral equation can be reduced to a form suitable for dealing with the type of body shown in fig 2. This body consists of a forebody (with either a blunt or a sharp nose) over which the radius y varies from zero up to a certain value at the shoulder. The afterbody is the region downstream of the shoulder where the radius remains constant and equal to the value at the shoulder. See Fig. 2.

Referring to equations 22, 26, 30, 31, 33, and 36 in Appendix B, the limit as the tail abscissa, x_1, tends to infinity is investigated.

The expression $g(x, t)$ (i.e. y^2 for the ellipsoid which cuts the body at $x = t$ and coincides at $x = x_o$ and x_1) reduces to

$$y^2 = g(x,t) \rightarrow \frac{f(t)\,(x-x_o)}{(t-x_o)} \quad \text{as } x_1 \rightarrow \infty$$

This is the equation of a paraboloid of revolution whose apex lies on the axis at $x = x_o$ and which cuts the body at $x = t$.

The length to diameter ratio, λ, of this degenerate ellipsoid, tends to infinity as $x_1 \rightarrow \infty$ (since it is then a paraboloid). Letting λ tend to infinity in the equation for the virtual mass coeficients, $k_1(\lambda)$ of the ellipsoid it is seen that

$$k_1(\lambda) \rightarrow 0 \qquad \text{as} \quad \lambda \rightarrow \infty$$

Similarly, k_o, the virtual mass coefficient of the ellipsoid cutting the body at $\frac{1}{2}(x_o + x_1)$ also tends to zero.

If $g(x, t)$ is now set equal to $\dfrac{f(t)\,(x-x_o)}{(t-x_o)}$,

the virtual mass coefficients set equal to zero, and x_1 equal to ∞ in equations 22, 26, 33, and 36 it is seen that

$$U_1(x) = \cos\gamma(x)$$

$$E_1(t) = -\frac{1}{2}\int_{x_o}^{\infty}\left[k(x,t) - k'(x,t)\right]dx$$

$$E_{n+1}(t) = E_n(t)\,E_1(t) - \frac{1}{2}\int_{x_o}^{\infty} k(x,t)\left[E_n(x) - E_n(t)\right]dx \qquad (n \geq 1)$$

$$U_{n+1}(t) = U_1(t) + \cos\gamma(t) \sum_{i=1}^{n} E_i(t)$$

At this point it would be possible to transform the region

$$x_0 \leq x \leq \infty \qquad \text{into} \qquad -1 \leq x' \leq 1$$

with

$$x' = \frac{x - 2x_0 - 1}{x - 1}$$

and perform one Gaussian quadrature over the whole region. However, due to the bunching of points near to the ends of the region of integration there will be very few points to define the region at the junction of forebody and afterbody. With no restriction we can say that the shoulder occurs at x = o and then we can split the integral up into two parts,

$$x_0 \leq x \leq 0 \qquad \text{and} \qquad 0 \leq x \leq \infty$$

If then each part of the integral is transformed into the region $-1 \leq x' \leq 1$, the total integral can be found by two Gaussian quadratures, one for the forebody and one for the after body. In this way points at which pressure is determined are bunched close together near the nose, $x = x_o$, and in the region of the shoulder, $x = o$, so defining these regions better.

The transformation for the forebody is given by

$$x' = 1 - 2(x/x_0)$$

and that for the afterbody is given by

$$x' = 1 - 2/(1+x)$$

Splitting up the integrals, performing the transformations shown above, and then writing x^1 as x again, the expression for $E_1(t)$ becomes

$$E_1(t) = \frac{x_0}{4}\int_{-1}^{+1}\left[k(x,t) - k'(x,t)\right]dx - \int_{-1}^{+1}\left[\frac{k(x,t) - k'(x,t)}{(1-x)^2}\right]dx$$

In a similar way the expression for $E_{n+1}(t)$ becomes

$$E_{n+1}(t) = E_n(t)E_1(t) + \frac{X_0}{4}\int_{-1}^{+1} k(x,t)\left[E_n(x) - E_n(t)\right]dx - \int_{-1}^{+1} k(x,t)\left[\frac{E_n(x)-E_n(t)}{(1-x)^2}\right]dx$$

The programme for the solution of these four equations is listed in Appendix D.

Input arrangements and layout of results

As in the case of the closed body, dealt with in the previous section the number of Gaussian abscissa is kept constant in order to simplify programme handling. It was decided to take the total number of abscissae over the whole body as 60 with 30 on the forebody and 30 on the afterbody. It has been found necessary to use as many as 30 points on the afterbody. This provides a lot of points close to the junction, but does not waste time by evaluating the velocity at a lot of points well downstream where pressure recovery to ambient is well established. The computation is halted when the maximum error function $E_n(t)$ is less than prescribed value. Convergence is slightly slower in this programme than in that for the closed body. If the maximum value of the error function is 10^{-3} then convergence will be achieved in a very short time. A value of 10^{-4}, on several of the bodies tested, caused run times to convergence to be about one or two minutes.

A subroutine has been built into the programme to evaluate y and dy/dx at each body abscissa, just as for the closed body.

The data to be supplied now consists of four numbers.

(i) NMAx- the maximum number of iterations permitted (used as a safeguard should convergence not be achieved or be slower than expected)
A typical value is 100.

(ii) EPS - convergence is achieved only if $|\max\{E_n(t)\}|$ is less than EPS. A typical value is 0.0005.

(iii) xxo - the nose abscissa, x_o

(iv) yAFT - the value of y on the afterbody.

Example:- A hemisphere cylinder. Taking the sphere radius as unity, the data card consists of four numbers (the first being of type integer, the other three being real), each separated by a space.

100 0.001 -1.0 1.0

Two lines of FORTRAN are needed to form y and $\frac{dy}{dx}$ on the forebody. In this example they are

```
FB = SQRT (1.0-XB*XB)

F1B = -XB/FB
```

These are placed in the subroutine BODY

The output is identical in layout to that for the closed body, namely a statement of the number of iterations and maximum value of the error at the time the computation ceased. This is followed by five columns of 60 numbers, the values of x, y, dy/dx, U and C_p at the abscissae. The body geometry is output to 6 decimal places and the values of U and C_p are given to 4 places.

A Note on scaling

The distribution of points on the afterbody was given as

$$x = (1+x')/(1-x')$$

where x^1 are the Gaussian abscissa given in $-1 < x' < +1$
This, as seen earlier, causes x to lie in the range

$$0 < x < \infty$$

The transformation $x = k(1+x')/(1-x')$ where k is a constant would also transform x^1 in the range $-1 < x' < 1$ to x in the range $0 < x < \infty$. The value of k used will affect the distribution of values of x between o and ∞, that is the distribution of points on the afterbody. In the programme k is taken as unity. If the forebody length is taken to be unity this results in a similar distribution of points immediately on either side of the forebody/afterbody junction. This is a desirable situation and scaling the forebody in this way (if necessary) is thus likely to give most accurate results in the shortest time.

Results

a) Closed body programme

Since the initial guess for the iterative solution of the integral equation should be exact for ellipsoids, a check was first made to ensure that this was so. Three ellipsoids with axis ratios of 2, 1, $\frac{1}{2}$ were considered These all converged to the required solution in one iteration when the appropriate expressions for virtual mass coefficients of ellipsoids broadside-on and end-on were incorporated.

A 10% thick parabolic arc of revolution was next run. The solution converged with a maximum error of 10^{-5} in 20 seconds. The pressure distribution is given in fig 3. Results from linearized theory due to Spreiter reference 3 are also shown on the same figure. As is characteristic of linearized methods, the result of Spreiter underestimates the peak suction by a proportion roughly equal to the thickness/chord ratio of the body.

It was decided to run the programme for a body having a slope discontinuity. A 10% thick diamond of revolution symmetrical fore and aft was chosen. Fig 4 shows the pressure distribution for this body. The infinite suction predicted by potential theory at the slope discontinuity is, of course, never realized by a numerical scheme. However the tendency towards infinite suction can clearly be seen in the figure.

The final closed body considered was one without fore and aft symmetry. This body, given incorrectly in reference 2, has the form

$$y = \frac{3\sqrt{3}}{20}\sqrt{x}\,(1-x)$$

It is 20% thick and has a blunt nose and pointed tail. Fig 5 shows the chordwise variation of pressure coefficient obtained from the programme with a maximum error of 10^{-5} in 30 seconds.

b) Infinite afterbody programme

A body of revolution in the form of a three-stage rocket (see Fig 6) presents geometry sufficiently challenging to test any suggested theoretical or computer solution. Fig 7 shows the computed values of pressure coefficient over the region of interest obtained from the programme in $2\frac{1}{2}$ minutes with a maximum error of 10^{-4}. Also shown are experimental values of C_p from reference 4. The agreement obtained may be said to be suprisingly good.

A further test was provided by considering a shape having a forebody fineness ratio less than that of the 3-stage rocket, but of simpler geometry. Fig 8 shows the pressure distribution over such a body, namely an ellipsoid cylinder of axis ratio (a/b) = 2. Convergence to a smooth result was again achieved in a computer time of 1 minute with a maximum error of 10^{-4}.

Neither of the two above bodies have regions where the surface slope is negative. Fig 9 shows the pressure distribution over a configuration whose forebody consists of two circular arcs, of the same radius, joining with constant surface slope at 75% of the forebody length aft of the nose. A smooth pressure variation was obtained with a maximum error of 10^{-4} after nearly 6 minutes of computer time. However had the solution been halted earlier, a $2\frac{1}{2}$ minute run giving a maximum error of 5×10^{-3} would have produced pressures which could not be plotted apart from those obtained in the longer run.

Conclusions

The results of test runs of the two programmes have demonstrated their flexibility and range of application. The closed body programme is very fast and copes equally well with a blunt or pointed nose and tail. Fore and aft assymmetry also presents no further problems. Indeed, since Landweber's solution (ref 1) has been well established for several years, the tests carried out in the closed body case were mainly to check the accuracy of the computing. Test runs on the infinite afterbody programme demonstrated its capacity to deal with severe body geometry. Run times were somewhat longer than those of the closed body programme, but these could be reduced substantially with very little loss in accuracy.

Both programmes have been designed so as to require very little data preparation, by keeping the order of the Gaussian quadrature fixed and by supplying body data via a subroutine. The two programme listings should prove useful since neither appears to be available in the current literature.

References

No.	Author(s)	Title, etc.
1.	L. Landweber	The axially symmetric potential flow about elongated bodies of revolution. Rep. Taylor Model Basin Wash. 761. 1951.
2.	B. Thwaites	Incompressible Aerodynamics. (Oxford), pp.390. 1960.
3.	J. R. Spreiter and A. Y. Alksne	Slender-body theory based on approximate solution of the transonic flow equations. NASA TR R-2. 1959.
4.	-	The City University, Department of Aeronautics, final year project - private communication.
5.	C. E. Weatherburn	Advanced Vector Analysis (Bell and Sons, London.) pp.20. 1960.

Acknowledgement

The author wishes to thank Mr. M. M. Freestone for his critical comment in the compiling of this report.

List of Symbols

x	streamwise co-ordinate with the origin at the body nose
y	body radius
γ	angle between tangent to body surface and the x axis
s	distance around the body perimeter in a meridian plane, measured from the nose
x_o	nose abscissa } See fig 1
x_1	tail abscissa
P	semi-perimeter in a meridian plane
U	total fluid velocity on the body surface, non-dimensionalised by free-stream velocity
k_o, k_1	virtual mass coefficients
f	square of body radius ($= y^2$)
g	square of ellipsoid radius
λ	length/diameter ratio of ellipsoid
U_n	the nth approximation for U
E_n	the error in the nth approximation
C_p	the local pressure coeft ($= 1 - U^2$)

Appendix A - the integral equation

Let S be the surface of a body of revolution with its axis aligned to the free stream. If V is the region exterior to S and $\underline{F}$ is a vector quantity single valued and continuous in V and on S then the Divergence theorem, ref 5, states

$$\int_S \underline{F} \cdot d\underline{S} = \int_V \operatorname{div} \underline{F}\, dV$$

where dV is an element of volume V, and $d\underline{S} = \underline{n}\,dS$, with dS as an element of surface area of S and $\underline{n}$ as the outward unit normal to S

1) Putting $\underline{F} = \phi \nabla \omega$ yields

$$\int_S \phi \nabla\omega \cdot d\underline{S} = \int_V \left[\phi \nabla^2\omega + \nabla\phi \nabla\omega\right] dV \quad \text{---- 1.}$$

2) Putting $\underline{F} = \omega \nabla \phi$ yields

$$\int_S \omega \nabla\phi \cdot d\underline{S} = \int_V \left[\omega \nabla^2\phi + \nabla\omega \nabla\phi\right] dV \quad \text{---- 2.}$$

Forming the difference of equations 1 and 2 one obtains

$$\int_S \left[\phi \nabla\omega - \omega \nabla\phi\right] \cdot d\underline{S} = \int_V \left[\phi \nabla^2\omega - \omega \nabla^2\phi\right] dV \quad \text{---- 3.}$$

If ϕ and ω are harmonic in V, then this leads to the result

$$\int_S \left[\phi \nabla\omega - \omega \nabla\phi\right] \cdot d\underline{S} = 0$$

and since $d\underline{S} = \underline{n}\,dS$ this becomes

$$\int_S \phi \frac{d\omega}{dn} dS = \int_S \omega \frac{d\phi}{dn} dS \quad \text{---------- 4.}$$

Considered here is a body of revolution moving with unit velocity in the negative x direction. If ϕ is the potential from which the velocities are derived, then the boundary condition on the body of zero relative normal velocity is given by:

$$d\phi/dn = -\sin\gamma \quad \text{---------- 5.}$$

where γ is the angle between the tangent to the meridian curve and the x axis.
The boundary condition at infinity is $\phi = 0$ since the fluid is at rest there.
Also dS can be expressed as

$$dS = 2\pi y\, ds \quad \text{---------- 6.}$$

where ds is an element of the perimeter of the body.
Substituting equations 5 and 6 into equation 4 gives

$$\int_0^P \phi y \frac{d\omega}{dn} ds = -\int_0^P y\omega \sin\gamma\, ds \quad \text{---------- 7.}$$

where P is meridian plane semi-perimeter of the body.

Now ω is an arbitrary harmonic function being continuous and single valued in V and on S. If ω is set equal to some unspecified axisymmetric potential function, then it will be related to the corresponding stream function ψ by

$$y\frac{d\omega}{dn} = \frac{d\psi}{ds} \quad \text{---------- 8.}$$

since n and s are orthogonal.

Setting this expression for $d\omega/dn$ in the left hand side of equation 7 gives

$$\int_0^P \phi y \frac{d\omega}{dn} ds = \int_0^P \phi \frac{d\psi}{ds} ds$$

Integrating by parts yields

$$\int_0^P \phi y \frac{d\omega}{dn} ds = [\phi\psi]_0^P - \int_0^P \psi \frac{d\phi}{ds} ds \quad \text{---------- 9.}$$

Superimposing on the flow field a unit velocity in the positive x direction will reduce the body to rest and produce a steady flow problem. Using the convention that velocities are given by the negative gradient of the potential, the steady velocity potintial, $\phi_{st.}$, can be written as

$$\phi_{st} = \phi - x$$

Thus

$$\frac{d\phi_{st}}{ds} = \frac{d\phi}{ds} - \frac{dx}{ds}$$

If U is the total velocity on the body surface in the steady flow (with a unit velocity free stream), then

$$U = - d\phi_{st} / ds$$

Also $dx/ds = \cos\gamma$ and hence

$$U = - d\phi / ds + \cos\gamma \quad \text{---------- 10.}$$

Substituting for $d\phi/ds$ from equation 10 into equation 9 gives

$$\int_0^P \phi\gamma \frac{dw}{dn} ds = \left[\phi\psi\right]_0^P - \int_0^P \psi(\cos\gamma - U) ds \quad \text{--- 11.}$$

Since the left hand sides of equations 7 and 11 are equal, it follows that

$$-\int_0^P \gamma w \sin\gamma ds = \left[\phi\psi\right]_0^P - \int_0^P \psi(\cos\gamma - U) ds$$

Writing $dx = ds\cos\gamma$ and $dy = ds\sin\gamma$ gives

$$-\int_0^P \gamma w dy = \left[\phi\psi\right]_0^P - \int_0^P \psi dx + \int_0^P \psi U ds \quad \text{--- 12.}$$

$$\text{ie} \quad \int_0^P \psi U \, ds = \int_0^P (\psi \, dx - y\omega \, dy) - \left[\phi \, \psi\right]_0^P \quad \text{---- 12.}$$

Now since ω and ψ are corresponding axisymmetric potential and stream functions the following relations hold.

$$y \frac{\partial \omega}{\partial x} = -\frac{\partial \psi}{\partial y} \quad \text{-- 13.} \qquad \text{and} \qquad y \frac{\partial \omega}{\partial y} = \frac{\partial \psi}{\partial x} \quad \text{---- 14.}$$

Equation 13 can be satisfied by the introduction of a function Ω such that

$$\psi = \frac{\partial \Omega}{\partial x} \quad \text{--- 15.} \qquad \text{and} \qquad -y\omega = \frac{\partial \Omega}{\partial y} \quad \text{---- 16.}$$

Thus we see that the integrand $(\psi dx - y\omega dy)$ occurring in equation 12 is an exact differential $d\Omega$.

When equations 15 and 16 are substituted into the relation 14., the resulting equation for Ω is

$$\frac{\partial^2 \Omega}{\partial x^2} + \frac{\partial^2 \Omega}{\partial y^2} = \frac{1}{y} \frac{\partial \Omega}{\partial y} \quad \text{------- 17.}$$

which is the equation satisfied by Stokes stream function.

Writing equation 12 in terms of Ω , gives

$$\int_0^P U \frac{\partial \Omega}{\partial x} \, ds = \left[\Omega - \phi \frac{\partial \Omega}{\partial x}\right]_0^P \quad \text{---- 18.}$$

Now setting Ω equal to a particular stream function, namely that of a source of unit strength situated at an arbitary point, t, on the axis of symmetry of the body

$$\Omega = (x-t)/r - 1 \qquad \text{where} \qquad r = \left[(x-t)^2 + y^2\right]^{1/2}$$

Thus

$$\frac{\partial \Omega}{\partial x} = \frac{y^2}{r^3}$$

Substituting this into equation 18 gives

$$\int_0^P \frac{U(x)\, y^2(x)\, ds}{r^3_{(x,t)}} = \left[\frac{x-t}{r(x,t)} - 1 - \frac{\phi\, y^2(x)}{r^3(x,t)} \right]_0^P = 2$$

Since y vanishes at s = o and s = P.

Thus the integral equation for velocity is given by

$$\int_0^P \frac{U(x)\, y^2(x)\, ds}{2r^3(x,t)} = 1 \qquad \text{---------- 19.}$$

Appendix B - the iterative solution

Successive approximations are used to solve the integral equation

$$\int_0^P \frac{U(x)\,y^2(x)\,ds}{2r^3(x,t)} = 1 \qquad \text{---------19.}$$

To obtain a first approximation, we make the polar transformation

$$x - t = y(x)\cot\theta$$

which reduces equation 19 to the form

$$\int_0^\pi \frac{U(x)\sin^2\theta\,d\theta}{2\sin[\theta-\gamma(x)]} = 1 \qquad \text{---------20.}$$

Near x = t the integrand of equation 20 peaks sharply and so the majority of the contribution to the total integral occurs in this region. As a result of this, a reasonable first approximation could be obtained by writing $U(x) = U(t)$. Also since $\gamma(x)$ will be small (except near the ends of the body) a further simplification is

$$\sin[\theta-\gamma(x)] \triangleq \sin\theta\cos\gamma(x) \triangleq \sin\theta\cos\gamma(t)$$

Inserting the two approximations into equation 20 gives

$U(t) = \cos\gamma(t)$ for each point t on the body.

i.e. $U(x) = \cos\gamma(x)$ is a first approximation.

An improved first approximation can be obtained as the velocity distribution over an ellipsoid of the same length and having a diameter equal to that of the body at its mid point. To justify this we must look at the relation between the virtual mass coefficient of a body and its velocity. For a body moving with unit velocity in the negative x direction the virtual mass equals twice the kinetic energy of the fluid.

i.e. $2T = k_o \Delta$ where Δ is the volume of the body.

and k_o is the virtual mass coeft.

$$k_o\Delta = 2T = -\rho\int\phi\frac{\partial\phi}{\partial n}dS = 2\pi\rho\int_0^P y\phi\sin\gamma\,ds$$

using equations 5 and 6. This is now integrated by parts.

$$k_0\Delta = \bar{\pi}\rho \int_{s=0}^{s=P} \phi\, d(y^2) = \bar{\pi}\rho\left[\phi y^2\right]_0^P - \bar{\pi}\rho \int_0^P y^2 \frac{d\phi}{ds}\, ds$$

$$\text{i.e.}\quad k_0\Delta = -\bar{\pi}\rho \int_0^P y^2 \frac{d\phi}{ds}\, ds = -\bar{\pi}\rho \int_0^P y^2 (\cos\gamma - U)\, ds$$

$$k_0\Delta = \bar{\pi}\rho \int_0^P U(x)\, y^2(x)\, ds - \Delta$$

$$\therefore \quad \Delta(1+k_0) = \bar{\pi}\rho \int_0^P U(x)\, y^2(x)\, ds \qquad \text{---------- 21.}$$

Consider a generalisation of the first approximation of the form

$$U(x) = C\cos\gamma(x)$$

then on substitution into equation 19.

$$C = 1+k_0$$

$$\text{i.e.}\quad U_1(x) = (1+k_0)\cos\gamma(x) \qquad \text{---------- 22.}$$

which is a better approximation.

However since k_0 is not known for the body under consideration, the value for the ellipsoid, having the same length and diameter as our body, is used.

By virtue of the above reasoning we see that the improved first approximation equation 22 is exact for an ellipsoid.

The position so far is that we wish to solve

$$\int_0^P \frac{U(x)\, y^2(x)\, ds}{2r^3(x,t)} = 1$$

where $r^2(x,t) = (x-t)^2 + y^2(x)$ and $x = x(s)$

We have a first approximation $U_1(x) = (1+k_0)\cos\gamma(x)$

An iteration formula of the following form suggests itself.

$$U_{n+1}(t) = U_n(t) + \cos\gamma(t)\left[1 - \int_0^P \frac{U_n(x)\, y^2(x)\, ds}{2r^3(x,t)}\right] \quad \text{---23.}$$

The error at the nth iteration is given by

$$E_n(t) = 1 - \int_0^P \frac{U_n(x)\, y^2(x)\, ds}{2r^3(x,t)} \quad \text{-----24.}$$

Hence $E_n(t)\cos\gamma(t) = U_{n+1}(t) - U_n(t)$ ---------25.

and $U_{n+1}(t) = U_1(t) + \cos\gamma(t) \sum_{i=1}^{n} E_i(t)$ ------26.

Using equations 23 and 25

$$E_{n+1}(t) = E_n(t) - \frac{1}{2}\int_{x_0}^{x_1} \frac{E_n(x)\, y^2(x)}{r^3(x,t)}\, dx \quad \text{---27.}$$

where x_0 and x_1 are the nose & tail abscissae.

The method of solution is as follows. Obtain a first approximation $U_1(x)$ as given by equation 22. The corrisponding error $E_1(x)$ will be given by 24. $E_2(x)$ is then obtained from $E_1(x)$ using 27, and $U_2(x)$ from 26. Repeated use of equations 26 and 27 will eventually produce terms so small as to be neglected. At this stage $U_n(x)$ will be the velocity distribution to the designed degree of accuracy.

In the evaluation of $E_1(x)$ (using equation 24) and of En(x) ($n \geq 2$, using equation 27) numerical integrations have to be performed. Neither of these two integrals is well suited to numerical integration as it stands (especially for elongated bodies), since y^2/r^3 has a sharp peak in the neighbourhood of x = t. In the evaluation of $E_1(x)$ from equation 24 the difficulty is overcome by subtracting from the integrand an integrable function which peaks in a similar way at x = t. The resulting integrand is then more easily treated numerically.

Set $$k(x,t) = \frac{f(x)}{[(x-t)^2 + f(x)]^{3/2}} \quad \text{-------28.}$$

where k(x, t) is the kernel in equations 24 and 27 and $f(x) = y^2(x)$

The integrable kernel which is now subtracted is that of an ellipsoid

$$k'(x,t) = \frac{g(x,t)}{\left[(x-t)^2 + f(x)\right]^{3/2}} \qquad \text{---------29.}$$

where $g(x, t)$ is the value of y^2 for an ellipsoid whose ends coincide with those of the body and which cuts the body at $x = t$, namely.

$$g(x,t) = \frac{f(t)\,(x-x_0)(x_1-x)}{(t-x_0)(x_1-t)} \qquad \text{---------30.}$$

Both kernels $k(x, t)$ and $k^1(x, t)$ now peak at the same point, namely $x = t$, and peak to the same value since by equation 30

$$g(t,t) = f(t)$$

Since $K^1(x, t)$ is to be subtracted from the integrand a similar quantity must be added. This will now be evaluated.

The length to diameter ratio, λ , of the ellipsoid is given from equation 30 by

$$\lambda^2 = \frac{(t-x_0)(x_1-t)}{f(t)}$$

and its virtual mass coefficients are given by:

$$K_1(\lambda) = \frac{\lambda \ln\left(\lambda + \sqrt{\lambda^2-1}\right) - \sqrt{\lambda^2-1}}{\lambda^2\sqrt{\lambda^2-1} - \lambda \ln\left(\lambda + \sqrt{\lambda^2-1}\right)} \qquad \text{for } \lambda > 1$$

$$K_1(\lambda) = 0.5 \qquad \text{for } \lambda = 1$$

$$K_1(\lambda) = \frac{\sqrt{1-\lambda^2} - \lambda^2 \ln\left[\frac{1+\sqrt{1-\lambda^2}}{\lambda}\right]}{2(1-\lambda^2)^{3/2} - \sqrt{1-\lambda^2} + \lambda^2 \ln\left[\frac{1+\sqrt{1-\lambda^2}}{\lambda}\right]} \qquad \text{for } \lambda < 1$$

---------31.

Consider the evaluation of $E_1(x)$ from $U_1(x)$ using equation 24.

$$E_1(t) = 1 - \int_0^P \frac{U_1(x)\, y^2(x)\, ds}{2r^3(x,t)} = 1 - \int_0^P \frac{U_1(x)\, k(x,t)\, ds}{2}$$

$$E_1(t) = 1 - \int_0^P \frac{U_1(x)}{2}\left[k(x,t) - k'(x,t)\right] - \int_0^P \frac{U_1(x)\, k'(x,t)\, ds}{2}$$

Now $U_1(x) = (1+k_0)\cos\gamma(x)$ as given by equation 22, and so

$$E_1(t) = 1 - \left(\frac{1+k_0}{2}\right)\int_{x_0}^{x_1}\left[k(x,t) - k'(x,t)\right]dx - \left(\frac{1+k_0}{2}\right)\int_{x_0}^{x_1} k'(x,t)\, dx \quad \text{--32.}$$

However, it is known that $U(x) = \left[1+k_1(t)\right]\cos\gamma(x)$ is an exact solution of the integral equation for the ellipsoid $g(x, t)$, therefore

$$\int_0^P \frac{\left[1+k_1(t)\right] k'(x,t)\cos\gamma(x)\, ds}{2} = 1$$

$$\text{i.e.} \quad \int_{x_0}^{x_1} k'(x,t)\, dx = 2 \,/\, \left(1+k_1(t)\right)$$

Substituting back into equation 32 gives

$$E_1(t) = 1 - \left(\frac{1+k_0}{2}\right)\int_{x_0}^{x_1}\left[k(x,t) - k'(x,t)\right]dx - \frac{1+k_0}{1+k_1(t)} \quad \text{---33.}$$

To evaluate the functions En(t) for $n \geq 2$ from equation 27 one must subtract an integrable function which peaks at the same position and by the same amount as does the existing integrand This is easily achieved by writing equation 27.in the form

$$E_{n+1}(t) = E_n(t) - \frac{1}{2}\int_{x_0}^{x_1} k(x,t)\left[E_n(x) - E_n(t)\right]dx - \frac{E_n(t)}{2}\int_{x_0}^{x_1} k(x,t)\,dx \quad \text{--- 34.}$$

However from equation 24 with n = 1 and $U_1(x) = (1+k_0)\cos\gamma(x)$ it follows that

$$E_1(t) = 1 - \frac{1+k_0}{2}\int_{x_0}^{x_1} k(x,t)\,dx$$

Thus

$$\int_{x_0}^{x_1} k(x,t)\,dx = \frac{2\left(1 - E_1(t)\right)}{1+k_0} \quad \text{--- --- --- 35.}$$

Substitute this back into equation 34 giving

$$E_{n+1}(t) = E_n(t) - \frac{1}{2}\int_{x_0}^{x_1} k(x,t)\left[E_n(x) - E_n(t)\right]dx - E_n(t)\left[\frac{1 - E_1(t)}{1+k_0}\right]$$

which can be written as

$$E_{n+1}(t) = E_n(t)\left[\frac{E_1(t)+k_0}{1+k_0}\right] - \frac{1}{2}\int_{x_0}^{x_1} k(x,t)\left[E_n(x) - E_n(t)\right]dx \quad \text{--- --- --- 36.}$$

Appendix C – listing of the programme for a closed body

```
    MASTER CLOSED BODY
    DIMENSION A (40),X(40),F(40),F1(40),E(40),E1(40),E2(40),1X1(40),U(40),CP(40),XK(40,40),
   F2(40)
    READ (1,1) NMAX,EPS,XXO,XX1,YMID
1   FORMAT (I0,4F0 0)
    A(1)=0 0045212771
    A(2)=0 0104982845
    A(3)=0 0164210584
    A(4)=0 0222458492
    A(5)=0 0279370070
    A(6)=0 0334601953
    A(7)=0 0387821680
    A(8)=0 0438709082
    A(9)=0 0486958076
    A(10)=0 0532278470
    A(11)=0 0574397691
    A(12)=0 0613062425
    A(13)=0.0648040135
    A(14)=0 0679120458
    A(15)=0 0706116474
    A(16)=0 0728865824
    A(17)=0 0747231691
    A(18)=0 0761103619
    A(19)=0 0770398182
    A(20)=0 0775059480
    X(1)=–0 9982377097
    X(2)=–0 9907262387
    X(3)=–0 9772599500
    X(4)=–0 9579168192
    X(5)=–0 9328128083
    X(6)=–0 9020988070
    X(7)=–0 8659595032
    X(8)=–0.8246122308
    X(9)=–0 7783056514
    X(10)=–0 7273182552
    X(11)=–0 6719566846
    X(12)=–0 6125538897
    X(13)=–0 5494671251
    X(14)=–0 4830758017
    X(15)=–0 4137792044
    X(16)=–0 3419940908
    X(17)=–0.2681521850
    X(18)=–0.1926975807
    X(19)=–0.1160840707
    X(20)=–0 0387724175
    DO 2 K=1,20
    KK=41–K
    A(KK)=A(K)
2   X(KK)=–X(K)
```

```
      DO 8 K=1,40
      X(K)=0 5*(X(K)*(XX1-XXO)+XX1+XXO)
      XB=X(K)
      CALL BODY (XB,FB,F1B)
      F(K)=FB
      F1(K)=F1B
      F2(K)=F1B
      X1(K)=(X(K)-XX0)*(XX1-X(K))
      F1(K)=1.0/SQRT(1 0+F1(K)*F1(K))
    8 F(K)=F(K)*F(K)
      XKO=XK1((XX1-XX0)/(2.0*YMID))
      DO 3 I=1,40
      FOFT=F(I)/X1(I)
      XL=SQRT(1 0/FOFT)
      XK2=(1.0+XKO)/(1 0+XK1(XL))
      SUM=0.0
      DO 4 J=1,40
      XDIF=(X(J)-X(I))*(X(J)-X(I))
      XK(I,J)=F(J)/SQRT((XDIF+F(J))**3)
      GXT=FOFT*XI(J)
      XKDASH=GXT/SQRT((XDIF+GXT)**3)
    4 SUM=SUM+A(J)*(XK(I,J)-XKDASH)
      E(I)=1 0-0 25*(1 0+XKO)*SUM*(XX1-XX0)-XK2
      E1(I)=(E(I)+XKO)/(1 0+XKO)
    3 U(I)=(1 0+XKO)*F1(I)
      N=0
    5 N=N+1
      DO 6 I=1,40
      U(I)=U(I)+F1(I)*E(I)
      SUM=0 0
      DO 7 J=1,40
    7 SUM=SUM+A(J)*XK(I,J)*(E(J)-E(I))
    6 E2(I)=E1(I)*E(I)--0.25*SUM*(XX1-XX0)
      DO 13 K=1,40
   13 E(K)=E2(K)
      EMAX=ABS(E(1))
      DO 2 K=1,40
      IF (ABS(E(K)) .GT. EMAX) EMAX=ABS(E(K))
   12 CONTINUE
      IF (EMAX GT EPS AND N LT NMAX) GO TO 5
      WRITE (2,14) N,EMAX
   14 FORMAT (20H NO OF ITERATIONS =,13,10X,13H MAX ERROR =,E15 7//)
      DO 9 K=1,40
      F(K)=SQRT(F(K))
    9 CP(K)=1 0-U(K)*U(K)
      WRITE (2,15)
   15 FORMAT (6X,2H X,13X,2H Y,12X,6H DY/DX,7X,9H VELOCITY,3X, 114H PRESS COEFT )
      WRITE (2,16) (X(K),F(K),F2(K),U(K),CP(K),K=1,40)
   16 FORMAT (F10 6,6X,F10 6,6X,F10 6,6X,F8 4,6X.F8 4)
      END
```

```
      FUNCTION XK1(B)
      IF (B  GT. 1 0001) GO TO 1
      IF (B  LT  0 9999) GO TO 2
      XK1=0 5
      RETURN
    1 C=B*B
      D=SQRT(C-1 0)
      E=ALOG(B+D)*B
      XK1=(E-D)/(C*D-E)
      RETURN
    2 C=B*B
      D=SQRT(1 0-C)
      E=ALOG((1 0+D)/B)*C
      XK1=(D-E)/(2 0*D*D*D-D+E)
      RETURN
      END



      SUBROUTINE BODY (XB,FB,F1B)

      RETURN
      END



      FINISH
```

Appendix D – listing of the programme for an infinite afterbody

```
      MASTER INFINITE AFTERBODY
      DIMENSION A(60),X(60),F1(60),E(60),E1(60).E2(60), 1U(60),F(60),CP(60),F2(60),XK(60,60)
      READ (1,1) NMAX,EPS,XXO,YAFT
    1 FORMAT (I0,3F0.0)
      A(1)=0 0079681925
      A(2)=0.0184664683
      A(3)=0 0287847079
      A(4)=0.0387991926
      A(5)=0 0484026728
      A(6)=0 0574931562
      A(7)=0.0659742299
      A(8)=0 0737559747
      A(9)=0 0807558952
      A(10)=0 0868997872
      A(11)=0 0921225222
      A(12)=0 0963687372
      A(13)=0 0995934206
      A(14)=0 1017623897
      A(15)=0.1028526529
      X(1)=–0 9968934841
      X(2)=–0 9836681233
      X(3)=–0 9600218650
      X(4)=–0 9262000474
      X(5)=–0 8825605358
      X(6)=–0.8295657624
      X(7)=–0,7677774321
      X(8)=–0.6978504948
      X(9)=–0 6205261830
      X(10)=–0 5366241481
      X(11)=–0.4470337695
      X(12)=–0.3527047255
      X(13)=–0.2546369262
      X(14)=–0 1538699136
      X(15)=–0 0514718426
      DO 2 K=1,15
      KK=31–K
      A(KK)=A(K)
    2 X(KK)=–X(K)
      DO 17 K=1,30
      KK=30+K
      A(KK)=A(K)
   17 X(KK)=X(K)
      DO 8 K=1,30
      X(K)=0 5*XX0*(1 0–X(K))
      XB=X(K)
      CALL BODY (XB,FB,F1B)
      F(K)=FB*FB
      F1(K)=1 0/SQRT(1 0+F1B*F1B)
      F2(K)=F1B
    8 A(K)=0 25*XX0*A(K)
      DO 14 K=31,60
      X(K)=(1.0+X(K))/(1 0–X(K))
      F(K)=YAFT*YAFT
```

```
   F1(K)=1 0
   F2(K)=0 0
14 A(K)=–0 25*(1 0+X(K))*(1 0+X(K))*A(K)
   DO 3 I=1,60
   FOFT=F(I)/(X(I)–XX0)
   E(I)=0 0
   DO 4 J=1,60
   XDIF=(X(J)–X(I))*(X(J)–X(I))
   XK(I,J)=F(J)/SQRT((XDIF+F(J))**3)
   GXT=FOFT*(X(J)–XX0)
   XKDASH=GXT/SQRT((XDIF+GXT)**3)
 4 E(I)=E(I)+A(J)*(XK(I,J)–XKDASH)
   E1(I)=E(I)
 3 U(I)=F1(I)
   N=0
 5 N=N+1
   DO 6 I=1,60
   U(I)=U(I)+F1(I)*E(I)
   E2(I)=E1(I)*E(I)
   DO 7 J=1,60
 7 E2(I)=E2(I)+A(J)*XK(I,J)*(E(J)–E(I))
 6 CONTINUE
   DO 13 K=1,60
13 E(K)=E2(K)
   EMAX=ABS(E(1))
   DO 12 K=1,60
   IF (ABS(E(K))  GT  EMAX) EMAX=ABS(E(K))
12 CONTINUE
   IF (EMAX  GT. EPS  AND  N  LT  NMAX ) GO TO 5
   WRITE (2,10) N,EMAX
10 FORMAT (20H NO  OF ITERATIONS =,I3,10X,13H MAX. ERROR =,E15 7//)
   DO 11 K=1,60
   F(K)=SQRT(F(K))
11 CP(K)=1 0–U(K)*U(K)
   WRITE (2,15)
15 FORMAT (6X,2H X,13X,2H Y,12X,6H DY/DX,7X,9H VELOCITY,3X,114H PRESS  COEFT )
   WRITE (2,16) (X(K),F(K),F2(K),U(K),CP(K),K=1,60)
16 FORMAT (F10 5,6X,F10 6,6X,F10.6,6X,F8 4,6X,F8 4)
   END




   SUBROUTINE BODY (XB,FB,F1B)

   RETURN
   END



   FINISH
```

Fig. 1

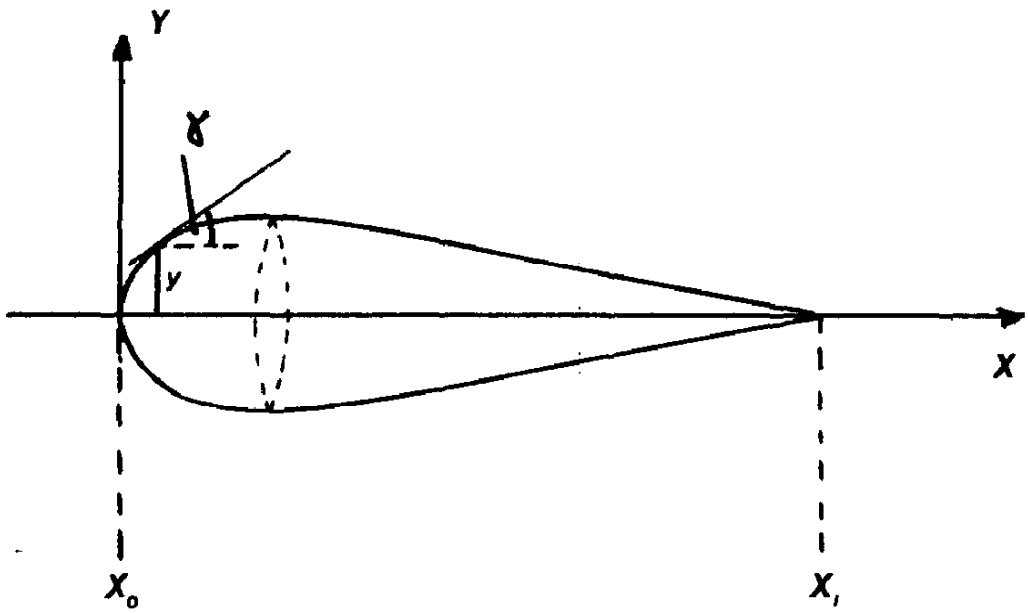

Closed body

Fig. 2

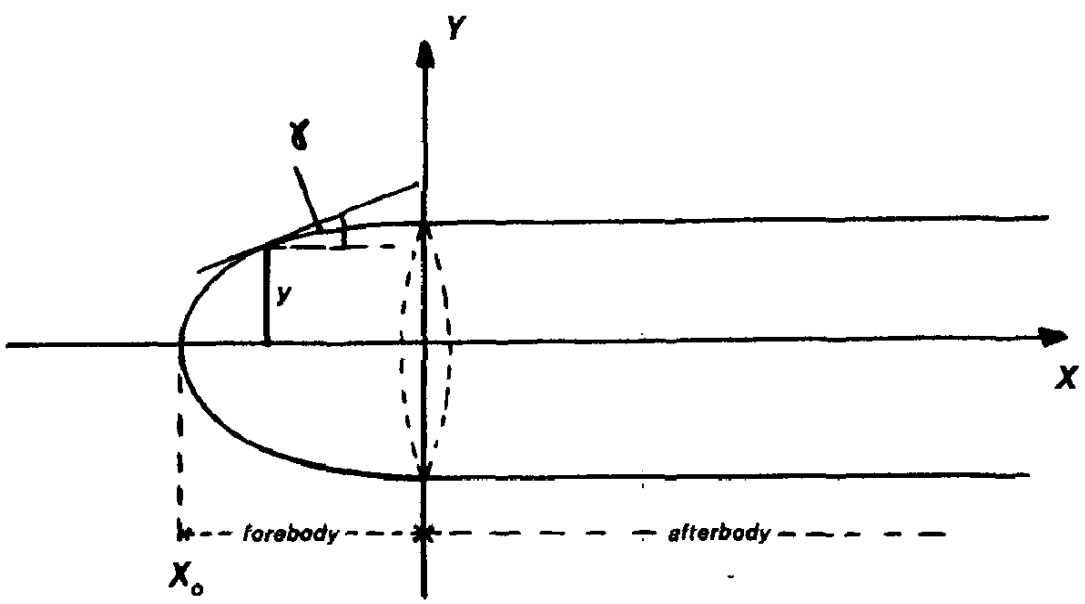

Body extending to infinity downstream

Fig. 3

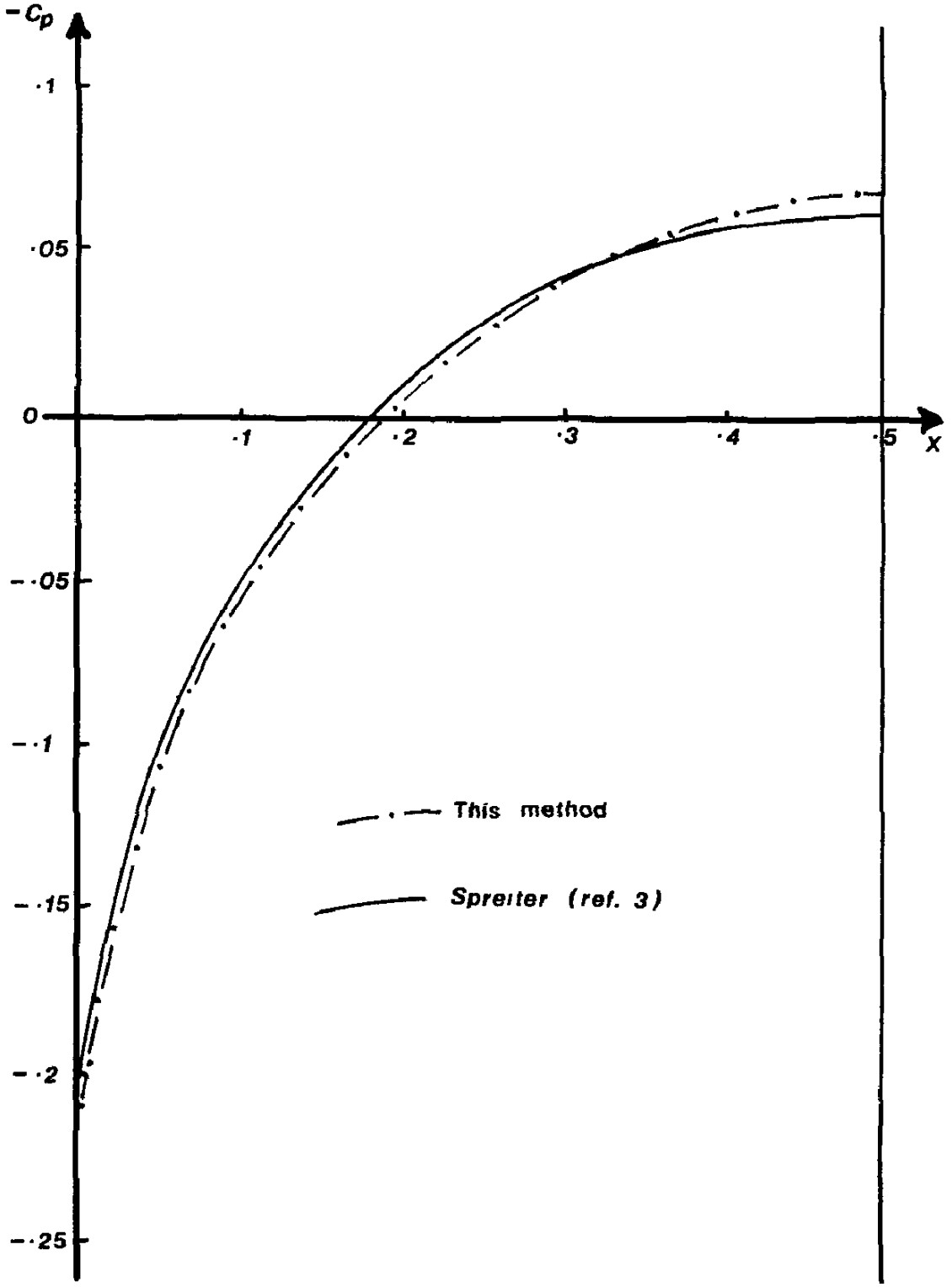

Pressure distribution on a 10% thick parabolic arc of revolution, $y = 0.2x(1-x)$

Fig.4

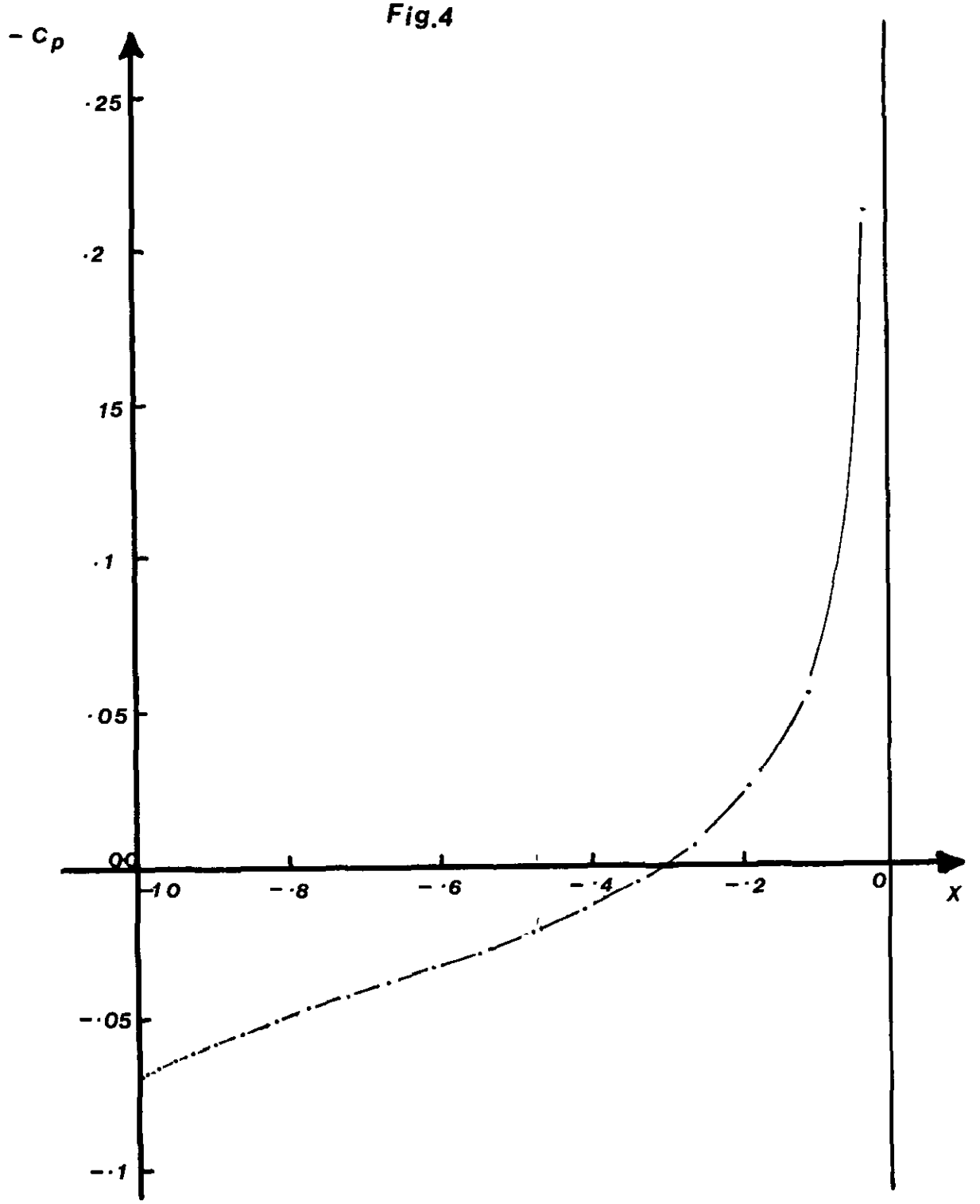

Pressure distribution on a 10% thick double cone

$y = 0{\cdot}1(1+x) \qquad -1 \leqslant x < 0$

$y = 0{\cdot}1(1-x) \qquad 0 < x \leqslant 1$

$y = 0{\cdot}1$ at $x = 0$

Fig. 8

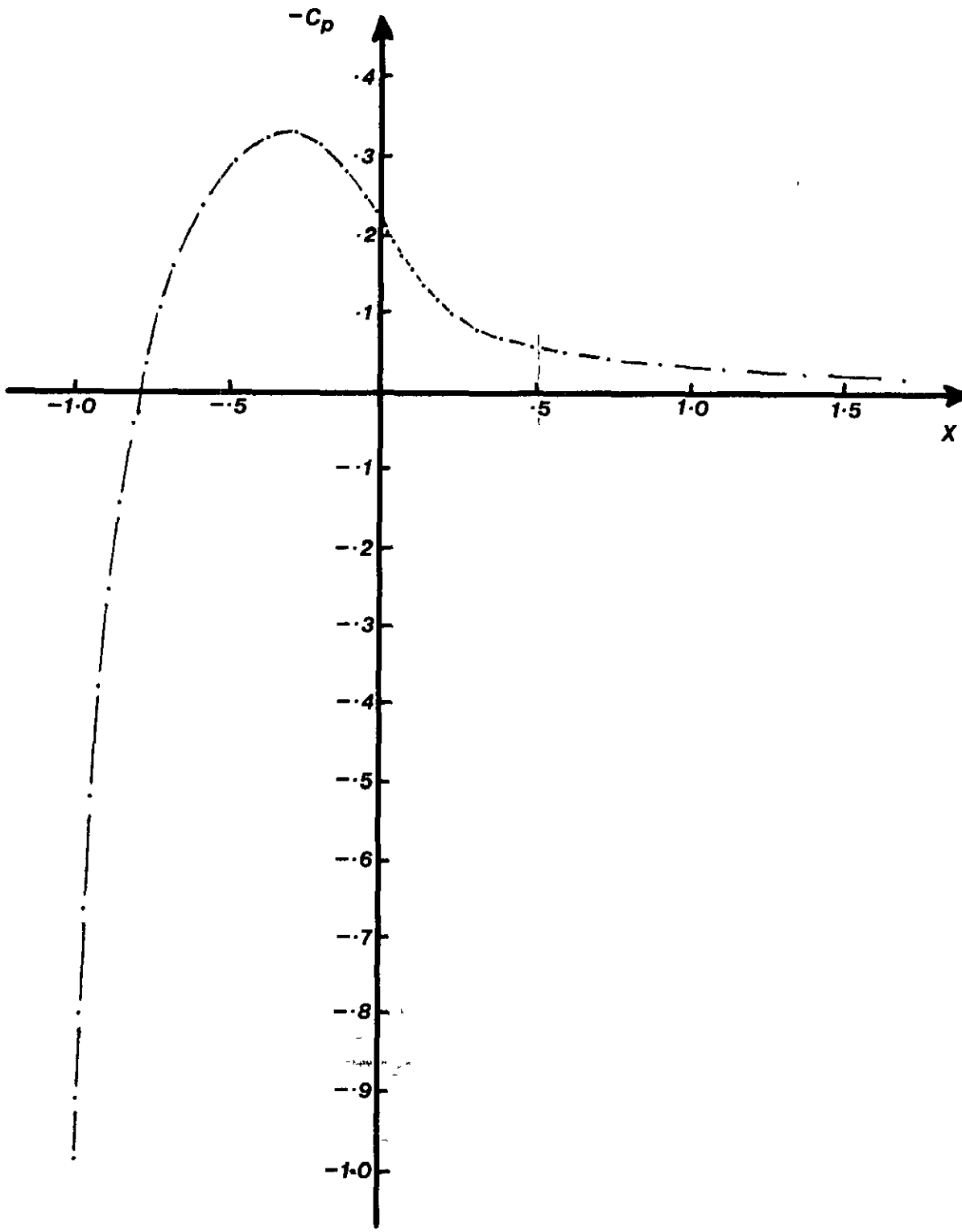

Pressure distribution on an elliptically headed cylinder

$x^2 + 4y^2 = 1$ $\quad -1 \leqslant x \leqslant 0$

$y = \cdot 5$ $\quad 0 < x$

Fig. 6

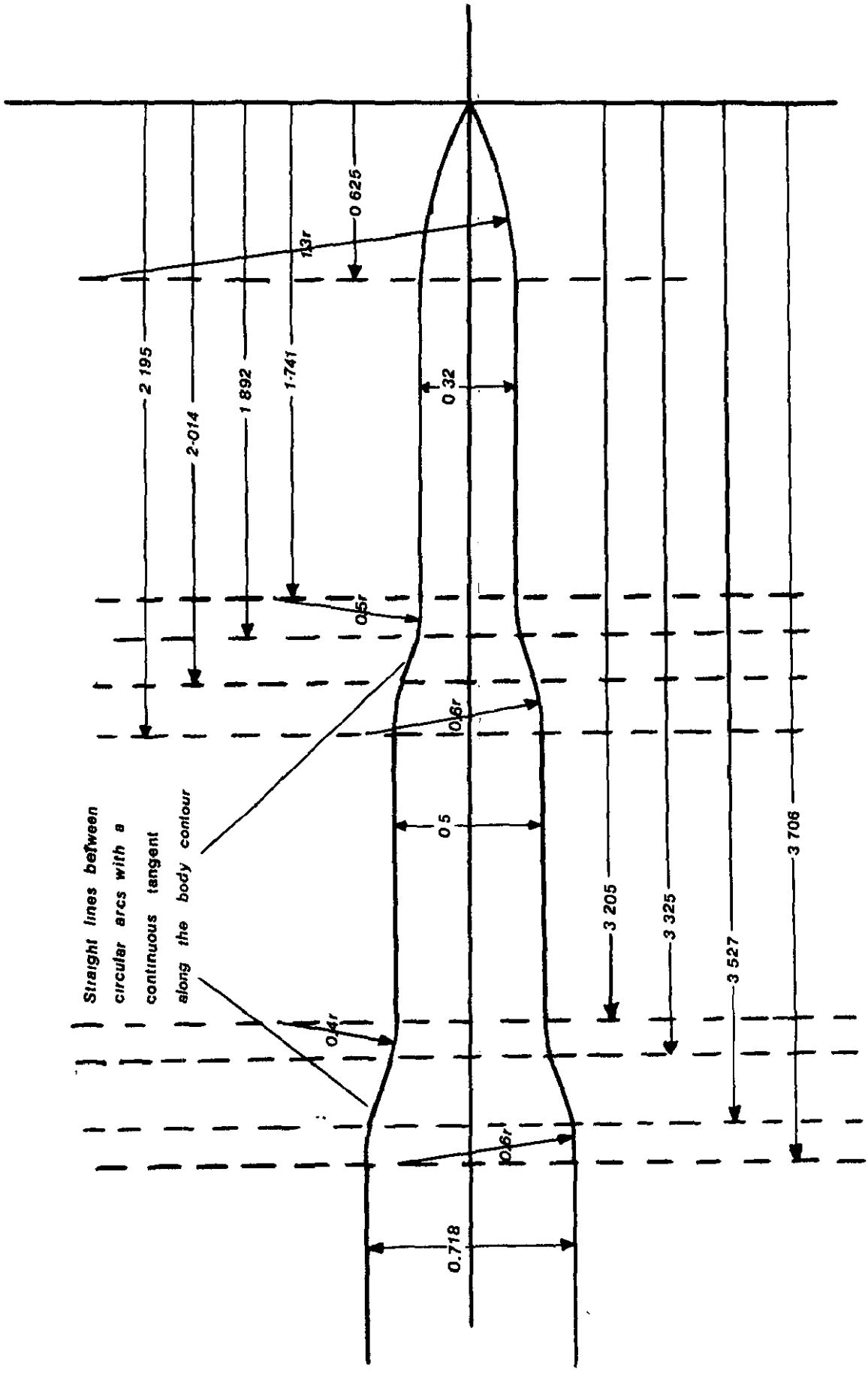
0 625
1,3r
2 195
2-014
1 892
1-741
0 32
0,5r
0,6r
0 5
3 205
3 325
3 527
3 706
Straight lines between circular arcs with a continuous tangent along the body contour
0,4r
0,6r
0.718

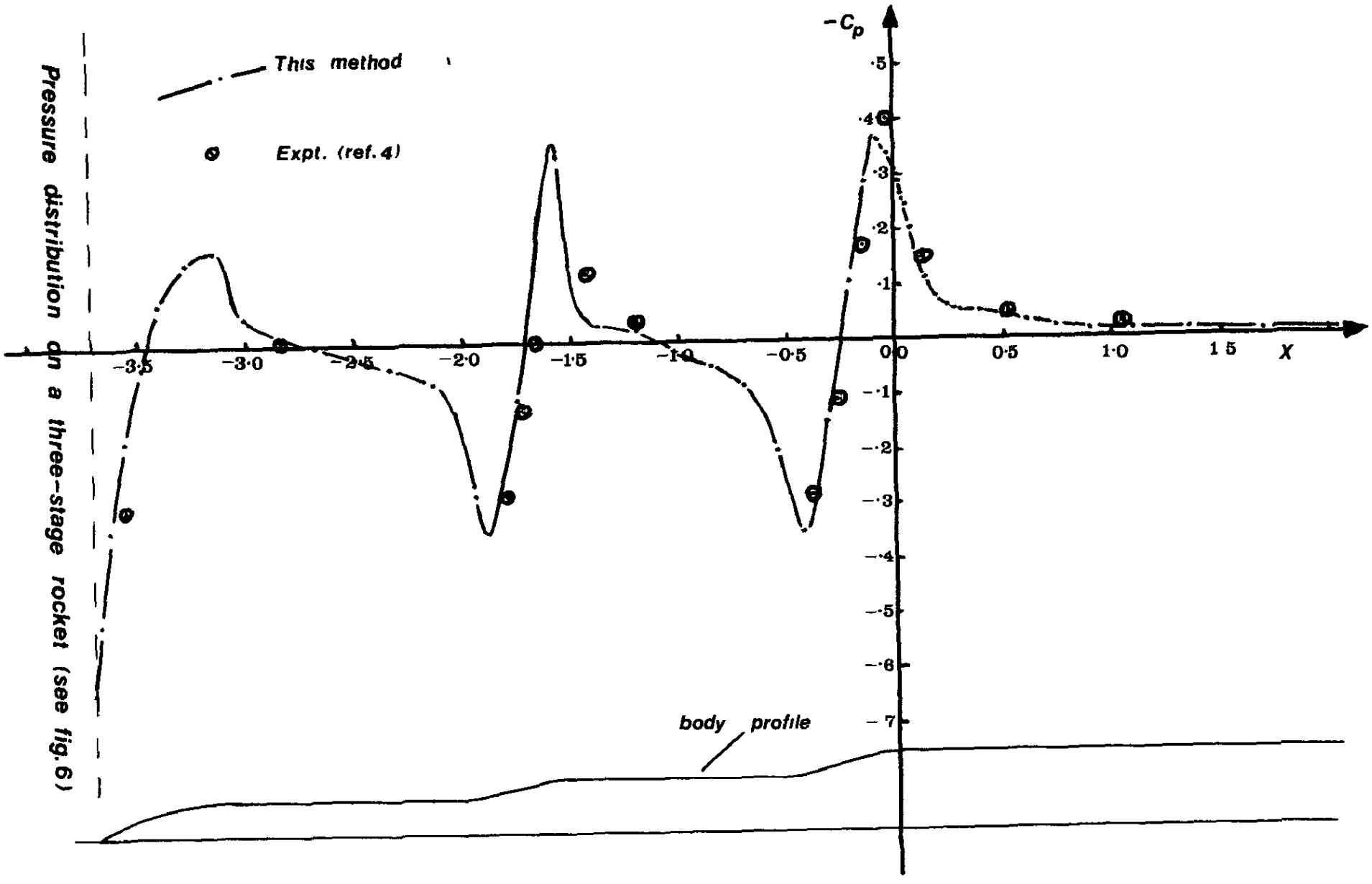

Fig. 7 Pressure distribution on a three-stage rocket (see fig. 6)

Fig. 8

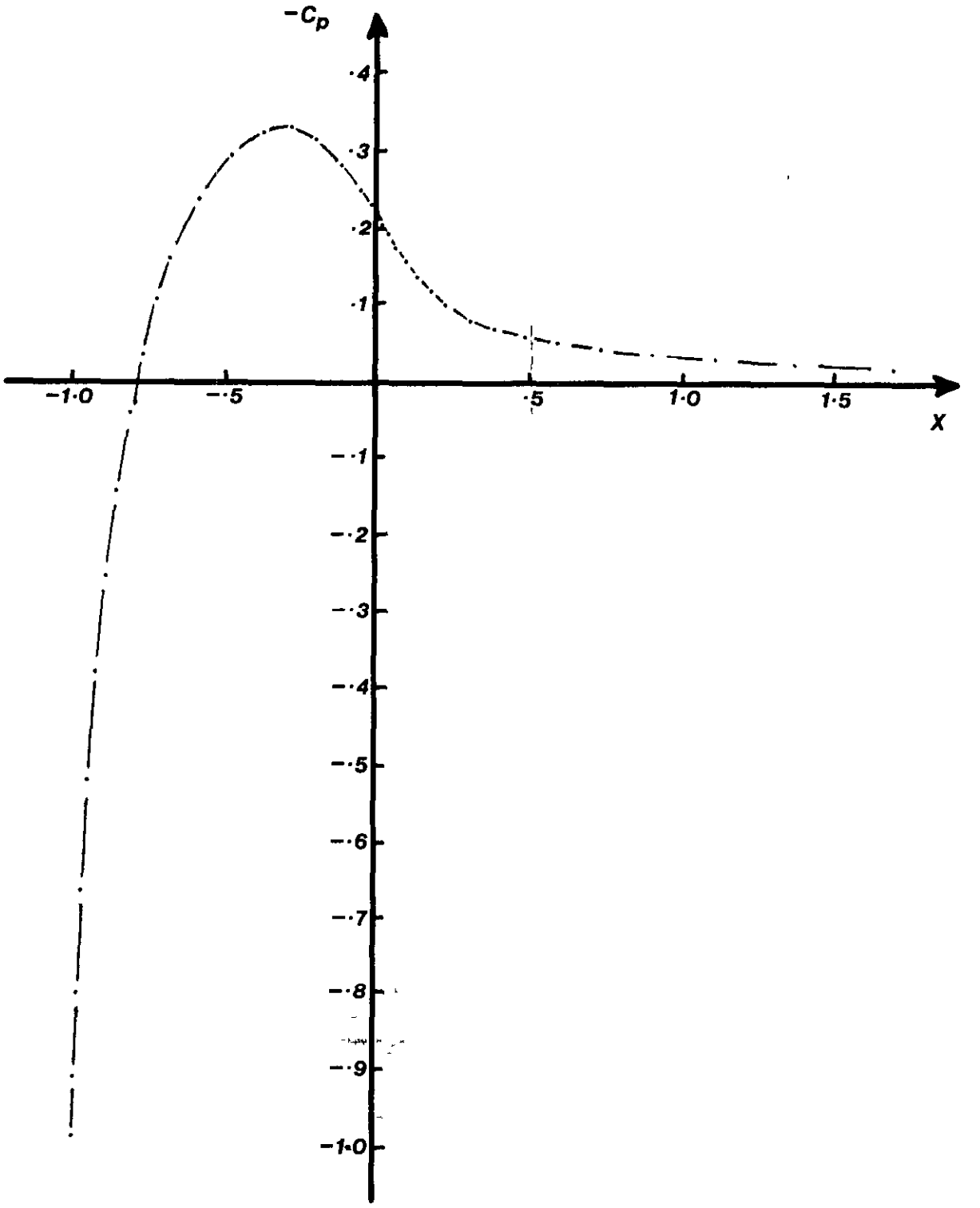

Pressure distribution on an elliptically headed cylinder

$x^2 + 4y^2 = 1$ $\quad -1 \leqslant x \leqslant 0$

$y = \cdot 5$ $\quad 0 < x$

Fig.9

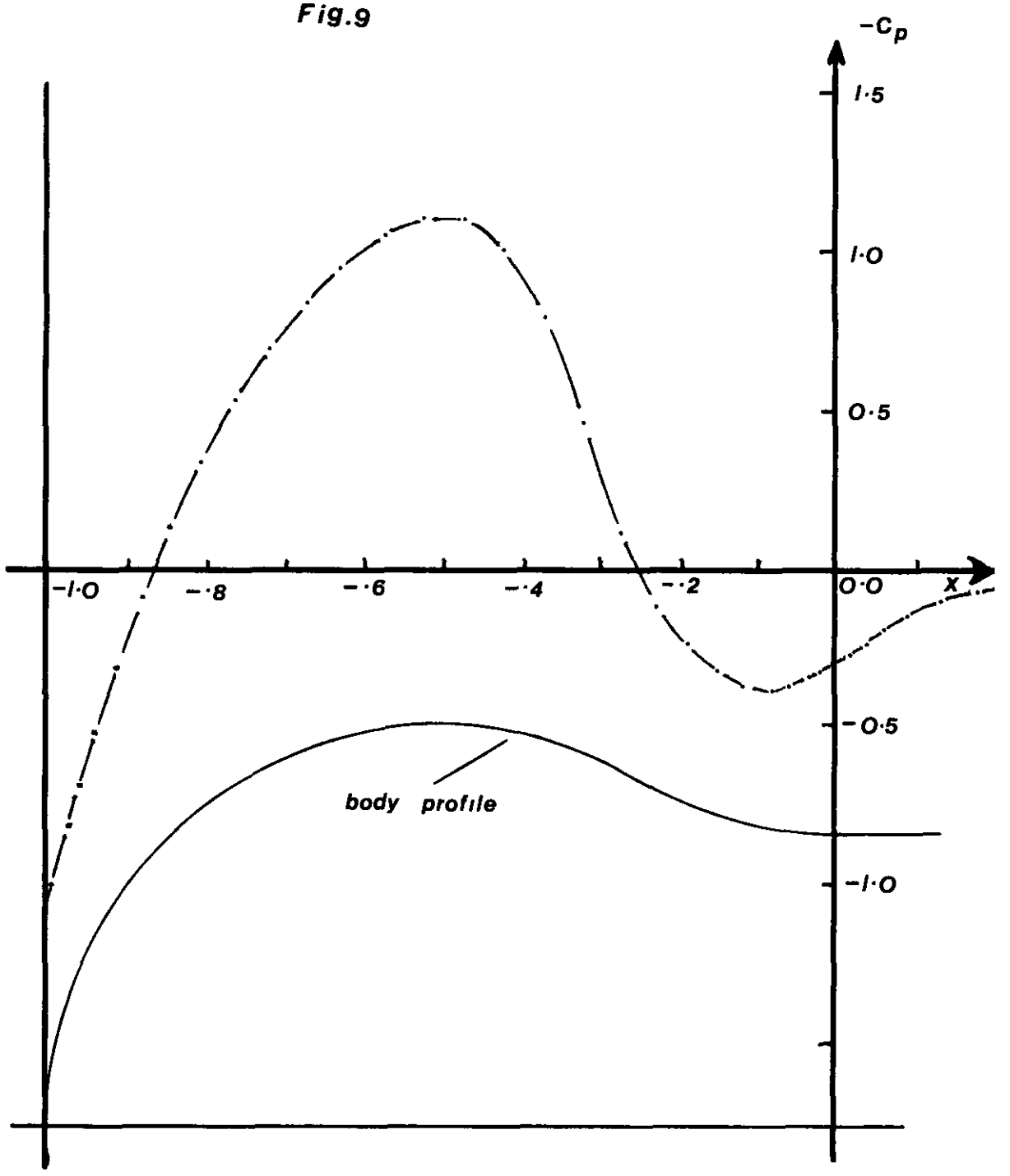

Pressure distribution on a body with negative slope on part of the forebody

HER MAJESTY'S STATIONERY OFFICE

Government Bookshops

49 High Holborn, London WC1V 6HB
13a Castle Street, Edinburgh EH2 3AR
109 St Mary Street, Cardiff CF1 1JW
Brazennose Street, Manchester M60 8AS
50 Fairfax Street, Bristol BS1 3DE
258 Broad Street, Birmingham B1 2HE
80 Chichester Street, Belfast BT1 4JY

Government publications are also available through booksellers

C.P. No. 1216

SBN 11 470774 X